ACS OMEGA

http://pubs.acs.org/journal/acsodf

Article

Evaluation of the Release Mechanism of Sustained-Release Tracers and its Application in Horizontal Well Inflow Profile Monitoring

Haitao Li, Zimin Liu,* Ying Li, Hongwen Luo, Xiaojiang Cui, Song Nie, and Kairui Ye

Cite This: *ACS Omega* 2021, 6, 19269−19280

Read Online

ACCESS | Metrics & More | Article Recommendations

ABSTRACT: The inflow profile is an important parameter to evaluate horizontal well productivity; however, quantitative interpretation of the inflow profile of the horizontal wells both accurately and cost-effectively is a common challenge faced by horizontal well production technology. The sustained-release chemical tracer is a new low-cost, long-lasting, and simple technique for monitoring the inflow profile in horizontal wells. In this study, a new type of sustained-release tracer is developed using bisphenol A-type epoxy resin as the polymer matrix and 2,6-difluorobenzoic acid, 3,4-difluorobenzoic acid, and 2,3,4,5-tetrafluorobenzoic acid as tracers. Meanwhile, the release mechanism and the influencing factors (chemistry of the tracer, temperature, salinity, and flow rate) of the sustained-release tracer are studied experimentally. The experimental results show that the release mechanism of the sustained-release tracer can be divided into two stages. The first stage involved the erosion process, in which the fluid gradually contacts and wraps the tracer, and the release rate is very fast. The second stage included the diffusion process, which is the diffusion−dissolution process once the fluid is completely wrapped around the tracer, and the release rate of this process is slow. The temperature is directly proportional to the release rate of the tracer, whereas salinity is inversely proportional to the release rate, and the fluid velocity does not affect the release rate. Finally, three kinds of sustained-release tracers are applied in the field, and a method to interpret the inflow profile of the sustained-release tracer is proposed. The result of application indicates that the sustained-release tracer developed in this study can efficiently monitor the inflow profile of the horizontal well.

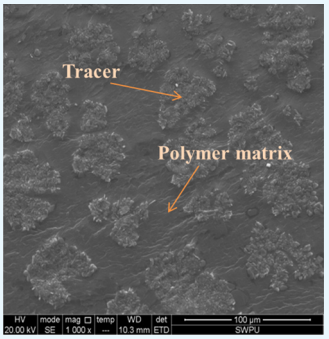

1. INTRODUCTION

With the continuous development in petroleum science and technology, a horizontal well plays an increasingly important role in oil/gas field production.[1] Compared to vertical wells, horizontal wells have the advantages of a shorter distance between wells, an extended well drainage area, increased critical coning flux, controlled injection fluid, and improved oil displacement efficiency. However, a reduction in the productivities of the wells due to an uneven distribution of the inflow profile along the wellbore resulting from the heterogeneity near the wellbore and drop in the pressure along the wellbore is the biggest disadvantage of horizontal wells, when applied to the heterogeneous reservoir in the oil/gas field.[2,3] Therefore, the main focus of horizontal well technology research has always been to discover and develop an efficient inflow profile monitoring approach.

At present, a few studies have proposed that the numerical simulation method can be used to predict the inflow profile;[4] however, the numerical simulation model requires a lot of reservoir parameters, which impacts the accuracy of the prediction results.[5,6] The conventional production logging tool is the most successful inflow profile testing method, but there are still some limitations of this approach.[7] For instance, the technology involves a one-time test that cannot be monitored over a long period and the requirement of a well-like structure that allows the test instrument to be run within the annulus makes it unsuitable for different types of horizontal wells.[8,9] The distributed temperature sensing is a newly developed technology that can monitor the real-time inflow profile.[10] However, due to the lack of accurate inversion approaches and the temperature measurement performance of fiber, it is difficult to accurately monitor the inflow profile.[11] The chemical tracer is an efficient monitoring technology with many useful applications in the oil and gas industry, including evaluation of the remaining oil saturation, waterflood optimization, and improving reservoir characterization, fluid pathways, and connectivity between wells.[12−16] With the development of chemical tracer technology, it is more and more widely used in a single-well test. Some scientists presented the application, implementation, and analysis of tracer flow back into unconventional reservoirs to determine the individual stage flow patterns and a qualitative correlation

Received: May 26, 2021
Accepted: July 9, 2021
Published: July 19, 2021

Table 1. Static Experimental Sampling Design

sample number	1	2	3	4	5	6	7	8	9	10	11	12
time (min)	10	20	40	60	120	180	300	420	690	960	1230	1500

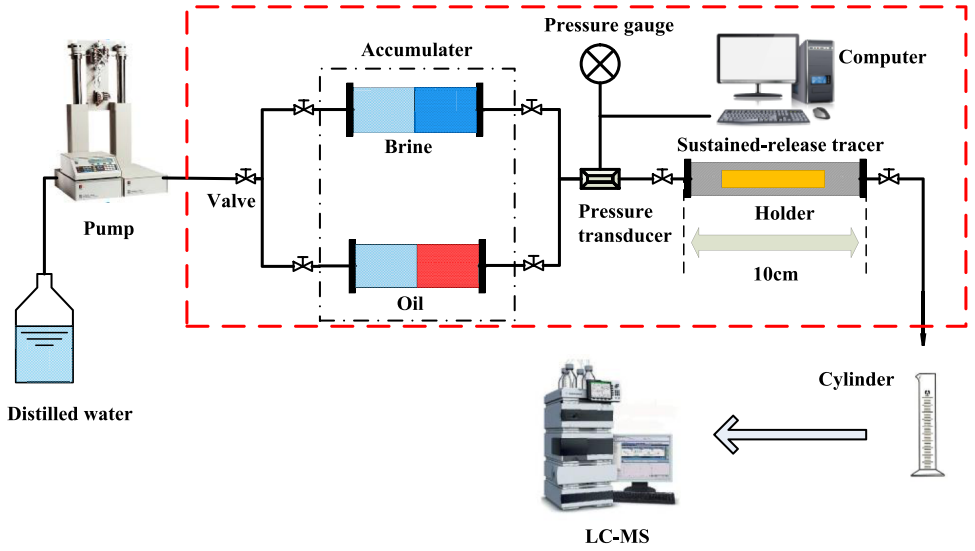

Figure 1. Dynamic experimental apparatus for the sustained-release tracer.

between the tracer flow back profiles and the complexity of the fracture networks.[17−20] In recent years, a new type of a downhole sustained-release tracer used for production monitoring is developed and applied in the horizontal wells.[21] The working principle of sustained-release tracers includes embedding a unique chemical tracer in a porous polymer matrix that can be released after contacting with sensitive fluid. The sustained-release tracers are placed in selected locations along the well to provide a permanent monitoring system, supplying information about[22] (1) the production zones, (2) the relative contribution of each zone, (3) the changes in the relative contribution of each zone over time, (4) the position of water breakthrough, and (5) the performance evaluation of the completion technology.

The initial purpose of the sustained-release tracer is to evaluate the effectiveness and performance of the ICD completions. Andresen et al.[23] applied the sustained-release tracer to monitor inflow profiles of offshore horizontal wells and described its working principle, installation, and the inflow profile interpretation method. Montes et al.[24] installed five water-soluble and oil-soluble tracers in the wellbore. The inflow profile and bottom water breakthrough time of the application well are obtained by tracer monitoring, thus verifying the effectiveness of the ICD completion. In addition, the sustained-release tracer is applied to the acid fracturing wells, and the results show that the inflow tracer can be adapted for acidification operations.[25] To improve the accuracy of interpretation results, an inflow profile interpretation model based on the tracer concentration distribution is proposed, and its reliability is verified in the application field.[26] Generally, conventional sustained-release tracers are soluble organic materials, which makes the detection more complicated. In order to reduce the tracer detection time, quantum dots are mixed with a polymer matrix to form a labeled tracer which has the characteristics of convenient detection. The quantitative and qualitative analysis of the quantum dot marker in the formation of fluid samples is carried out to evaluate the performance of the horizontal well production.[27] From what has been discussed above, the sustained-release tracer is a releasable solid-state tracer with strong adaptability, long timelines, high accuracy, and can be widely used in onshore and offshore oil fields.[28] However, the preparation methods, specific release mechanisms, and release rules have not yet been reported in detail.

In this study, according to the characteristics of sustained-release tracers, three kinds of water-soluble sustained-release tracers are developed, and their release mechanism and influencing factors are studied. First, three water-soluble tracers of fluorobenzoic acid (FBA)[29] (2,6-difluorobenzoic acid, 3,4-difluorobenzoic acid, and 2,3,4,5-tetrafluorobenzoic acid) and bisphenol-A type epoxy resin are selected for the preparation of three water-soluble sustained-release tracers and their release mechanisms are discussed. Second, the effects of temperature, fluid salinity, and flow rate on the release rate of these tracers are studied through static and dynamic experiments. Finally, the sustained-release tracers are applied in the field and the inflow profile of the test well is obtained by analyzing the tracer concentration distribution in the produced fluid.

2. EXPERIMENT

2.1. Laboratory Equipment and Drugs. *Drugs.* Bispheno1-A type epoxy resin, maleic anhydride, xylene, 2,6-difluorobenzoic acid, 3,4-difluorobenzoic acid, 2,3,4,5-tetrafluorobenzoic acid, pure acetonitrile, formic acid, hydrochloric acid, sodium hydroxide, and pure water.

Laboratory Equipment. Thermostatic chamber, Teflon mold, electric heating mixer, Teflon stirring bar, ultra-high pressure liquid chromatography−mass spectrometer (UPLC-MS), chromatographic column (Agilent Eclipse Plus C_{18}, 2.1 × 50 mm, 1.8 μm), and ultracentrifuges.

2.2. Preparation of the Sustained-Release Tracer. Three portions of 100 g bisphenol A epoxy resin were weighed and put into beakers and then heated in a thermostat at 120 °C

https://doi.org/10.1021/acsomega.1c02748
ACS Omega 2021, 6, 19269−19280

for 30 min. Later, they were put into an electric stirrer to adjust the temperature to 100 °C. 10 g of xylene was added to the epoxy resin and stirred evenly. Next, 50 g each of 2,6-difluorobenzoic acid, 3,4-difluorobenzoic acid, and 2,3,4,5-tetrafluorobenzoic acid tracers was added into the epoxy beaker and stirred at 500 r/min and 100 °C for 15 min until the mixture was fully mixed. Then, 35 g of curing agent maleic anhydride was added in each beaker containing the mixture and was continuously stirred thoroughly for 30 min at a stirring speed of 500 r/min. After stirring evenly, the epoxy resin−tracer mixture was poured into a Teflon mold and cured in a thermostat for 3 h. Finally, the solidified sustained-release tracer was removed from the mold for later use.

2.3. Static and Dynamic Release Experiments of the Sustained-Release Tracer. *Static Release Experiment.* The static experiment was conducted to evaluate sustained-release ability and influencing factors of the sustained-release tracer. The three prepared sustained-release tracers were addedto the beakers containing 1 L of water, and the beakers were kept under experimental conditions. Samples were taken out periodically. For 2 mL of each sample, 1 L of water was added to the beakers after withdrawing each sample. The specific sampling time of the experiment is shown in Table 1.

Dynamic Release Experiment. Dynamic experiments were conducted to evaluate the effect of different flow rates on the release rate of the sustained-release tracers. The experiment adopted the method of constant-flow injection pump displacement. By setting different flow rates (2, 6, and 10 mL/min), the influence of different flow rates on the release of the tracer at the same time was evaluated. The experimental device is shown in Figure 1.

Experimental operation steps are as follows: (1) The sustained-release tracer was put into the holder and the outlet valve was closed. (2) The speed constant current pump was started to adjust the flow rate. (3) When the pump pressure began to rise, this implied that the fluid filled the entire flow system. Now, the valve was opened for sampling. The specific sampling time was consistent with that in the static experiment, as shown in Table 1, and 2 mL of the sample was withdrawn each time.

2.4. Test Methods for the Tracer. FBA-based compounds do not exist in the formation fluids and have good thermodynamic and chemical stability and have gradually been applied in oilfield tracer testing technology.[30] Presently, the analytical methods used for tracer FBA compounds include gas chromatography−mass spectrometry, ion chromatography, high-performance liquid chromatography, and UV−visible spectroscopy. However, the above methods may have drawbacks such as complex sample processing process, slow analysis speed, and low detection sensitivity. Therefore, in the present study, UPLC-MS was used to establish the quantitative analysis of the FBAs. The chromatography and mass spectrometry were conducted under the following conditions:[31,32]

(1) Liquid chromatography conditions: An Agilent Eclipse Plus C_{18} column (2.1 × 50 mm, 1.8 μm) was used for the study. The mobile phase A was water and B was methanol. Gradient: 0−2 min, 3% B; 2.1−4 min, 20% B; 4.1−5 min, 90% B; and 5−8 min, 3% B. Flow rate: 0.4 mL/min. The injection volume was 2 μL, and the column temperature was set at 30 °C.

(2) Mass spectrometry conditions: An electrospray ion source, negative ion mode (ESI−), atomizer pressure (N_2) 20 psi, flow rate of dry gas (N_2) 10 L/min, drying temperature 350 °C, capillary voltage 3500 V, and mass scanning range m/z 100−500. The mass spectrum parameters were optimized according to the primary and secondary mass spectrum characteristics of each component, and the multi-reactive ion monitoring mode was used to determine the mass spectrum of each component as per the time segments.

3. RESULTS AND DISCUSSION

3.1. The Structure of the Sustained-Release Tracer. Figure 2 shows the circular cakes of the three types of the sustained-release tracer. It can be seen that the tracers are embedded in the polymer matrix. The three tracers selected are water-soluble with good thermal and chemical stability and are environment friendly.[31] The polymer matrix is a thermosetting material resistant to thermal decomposition at formation temperature and has good strength and toughness that allows it to withstand high-shear downhole fluids.

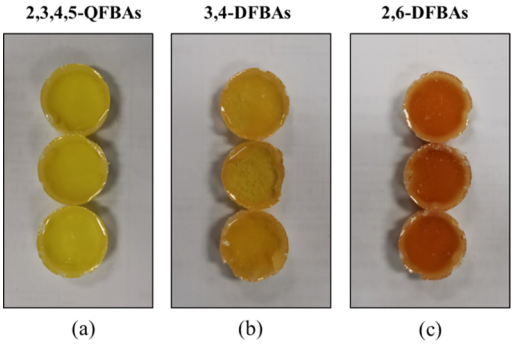

Figure 2. Sustained-release tracer material. (a) 2,3,4,5-tetrafluorobenzoic acid, (b) 3,4-difluorobenzoic acid, and (c) 2,6-difluorobenzoic acid.

Figure 3a depicts a 1000 times-magnified image of the sustained-release tracer surface topography and shows the presence of a lot of pores in the sustained-release tracer. Once the formation fluids enter the polymer matrix and contact the tracer in the pore, the tracers begin to release in the formation fluid. Figure 3b shows the microscopic image taken at a magnification of 5000 times. It showed that the tracer is evenly distributed in the matrix, which had a sufficient contact area with the formation fluids to ensure its complete release ability. Figure 3c shows the energy spectrum scanning results of the sustained-release tracer. The main elements of the sustained-release tracer are C, O, and F, consistent with the composition of the raw materials. From these results, it can be inferred that (1) there is no reaction between the polymer matrix and the formation fluid, (2) the tracer has good stability in the formation, (3) the polymer matrix shows good permeability, and (4) the tracer has single sensitivity (water solubility), high detection accuracy, non-local formation, and good stability.

3.2. Quantitative Detection of Sustained-Release Tracers. Figure 4 shows the liquid chromatographs of the three tracers, where the retention time of 2,6-difluorobenzoic acid, 3,4-DFBAs, and 2,3,4,5-tetrafluorobenzoic acid is around 10 min, 17 min, and 18 min, respectively. It can be seen that the chromatographic peaks of the three tracers exhibited

https://doi.org/10.1021/acsomega.1c02748
ACS Omega 2021, 6, 19269−19280

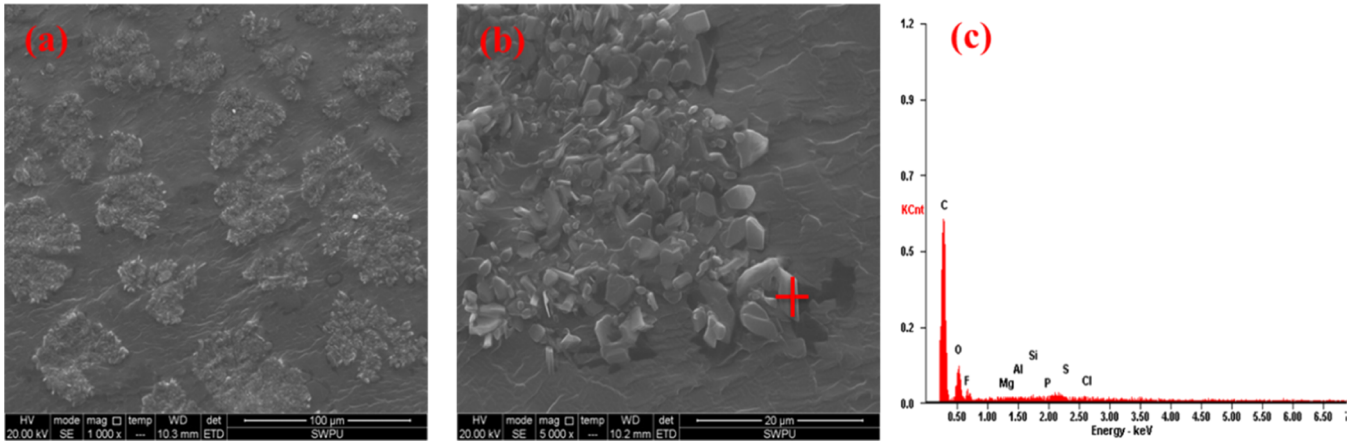

Figure 3. Micromorphology and the energy spectrum of the sustained-release tracer. (a) 1000 times. (b) 5000 times. (c) Energy spectrum.

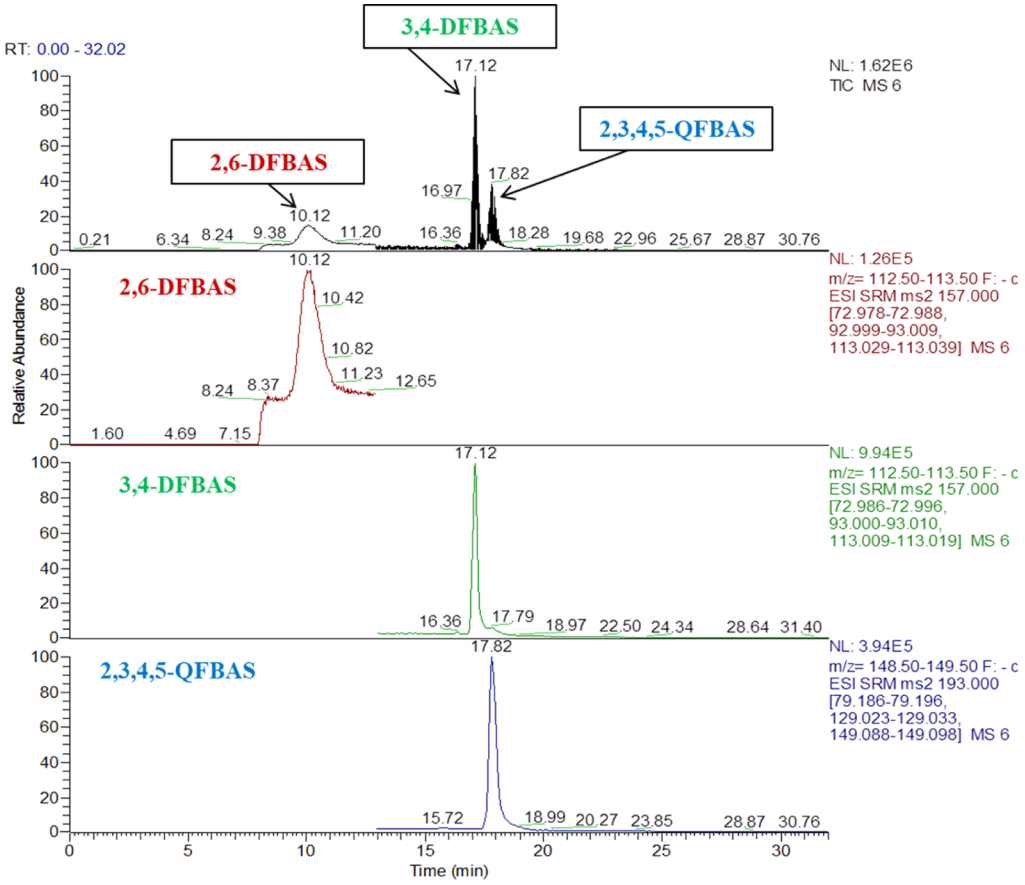

Figure 4. Detection of three FBA tracers by UPLC-MS (10 μL injection).

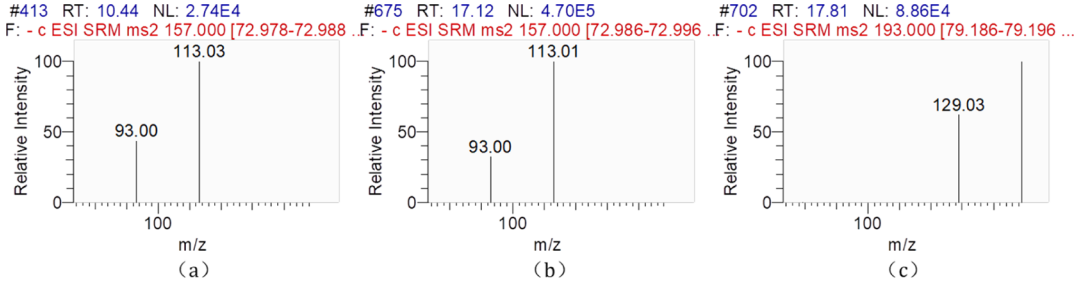

Figure 5. TIC total-ion flow profiles of the three FBA tracers.

https://doi.org/10.1021/acsomega.1c02748
ACS Omega 2021, 6, 19269−19280

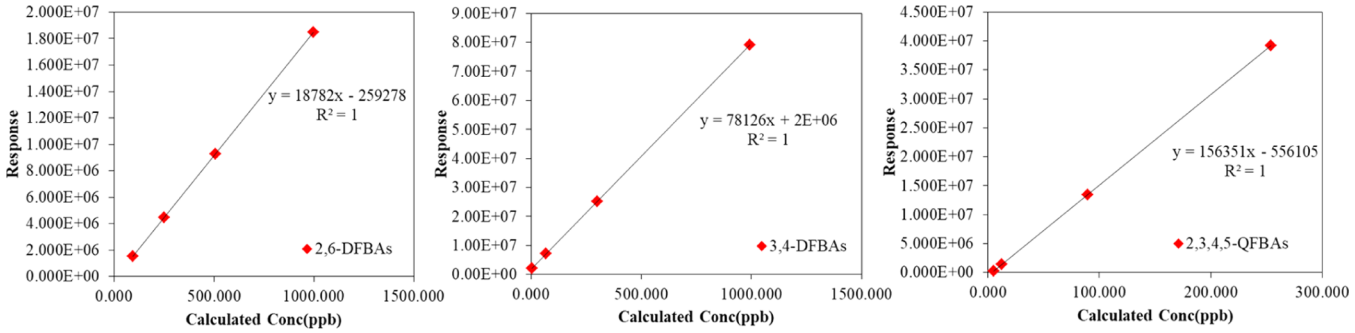

Figure 6. Standard working charts of the three tracers.

Table 2. Regression Equations and Correlation Coefficients of the Three Tracers

tracer	the regression equation	linear range (ppb)	R^2	LOD (ppb)	LOQ (ppb)	RSD (%)
2,3,4,5-tetrafluorobe-nzoic acid	$Y = -556105 + 156351 \times X$	1−1000	0.9961	0.033	0.17	0.64
2,6-difluorobenzoic acid	$Y = -259278 + 18782.2 \times X$	1−1000	0.9998	0.024	0.12	1.51
3,4-difluorobenzoic acid	$Y = 1.78006e + 006 + 78125.8 \times X$	1−1000	0.9942	0.032	0.1	0.8

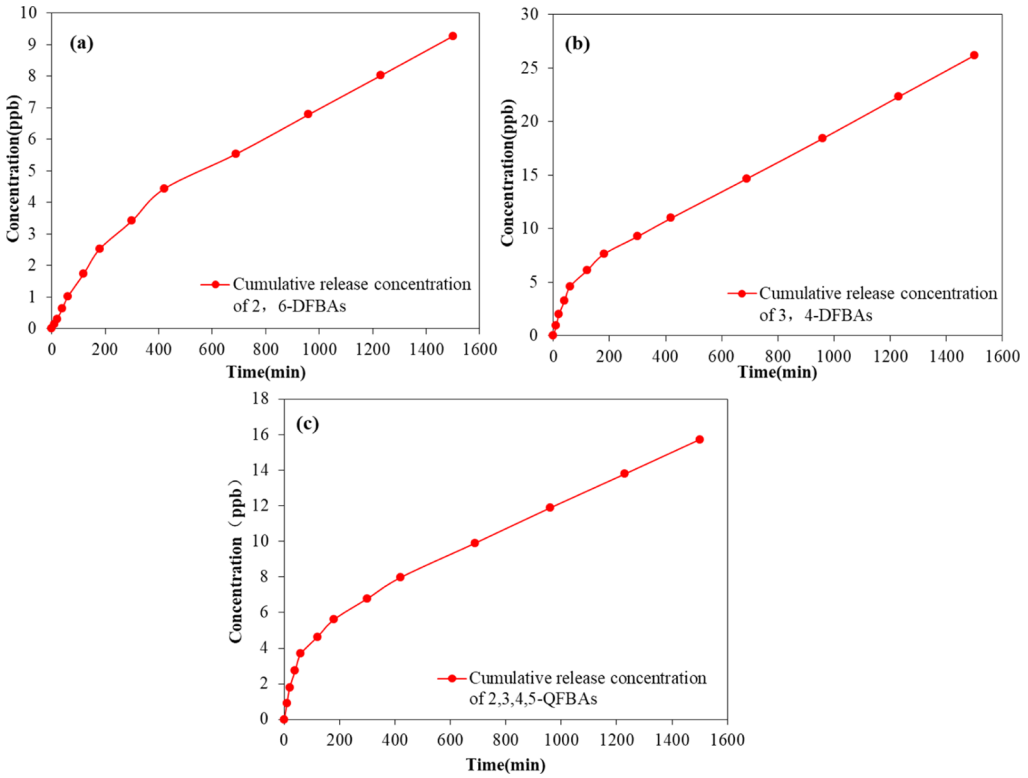

Figure 7. Cumulative release concentrations of three sustained-release tracers under static conditions. (a) 2,6-Difluorobenzoic acid, (b) 3,4-difluorobenzoic acid, and (c) 2,3,4,5-tetrafluorobenzoic acid.

obvious time intervals and significant peaks. Figure 5 shows the mass spectra conditioned with three different kinds of tracer-ion flow distribution. Because 3,4-difluorobenzoic acid and 2,6-difluorobenzoic acid have the same molecular weight, these two tracers have the same parent ion and daughter ion as 113.0 and 93.0, respectively. The parent ion and daughter ion of 2,3,4,5-tetrafluorobenzoic acid are 149.0 and 129.0, respectively. The specific peak values and high sensitivity of the test results can provide an effective separation and quantitative analysis of the three kinds of material.

Figure 6 shows the standard curve of the three tracers and Table 2 shows the linear range, regression equation, correlation coefficient, limit of detection (LOD), and the limit of quantification (LOQ) for the three tracers. As seen from the results provided in Table 2, the correlation coefficient R^2 of the standard working curves of the three tracers is greater than 0.99, indicating that the linear relationship of each substance is satisfactory within the quantitative linear range and the target compound can be accurately quantified. The precision test results show that the peak area root-square deviation (RSD) of the three tracers is less than 2% even after repeatedly conducting six runs of the same sample, indicating good tightness and repeatability of the method.

https://doi.org/10.1021/acsomega.1c02748
ACS Omega 2021, 6, 19269−19280

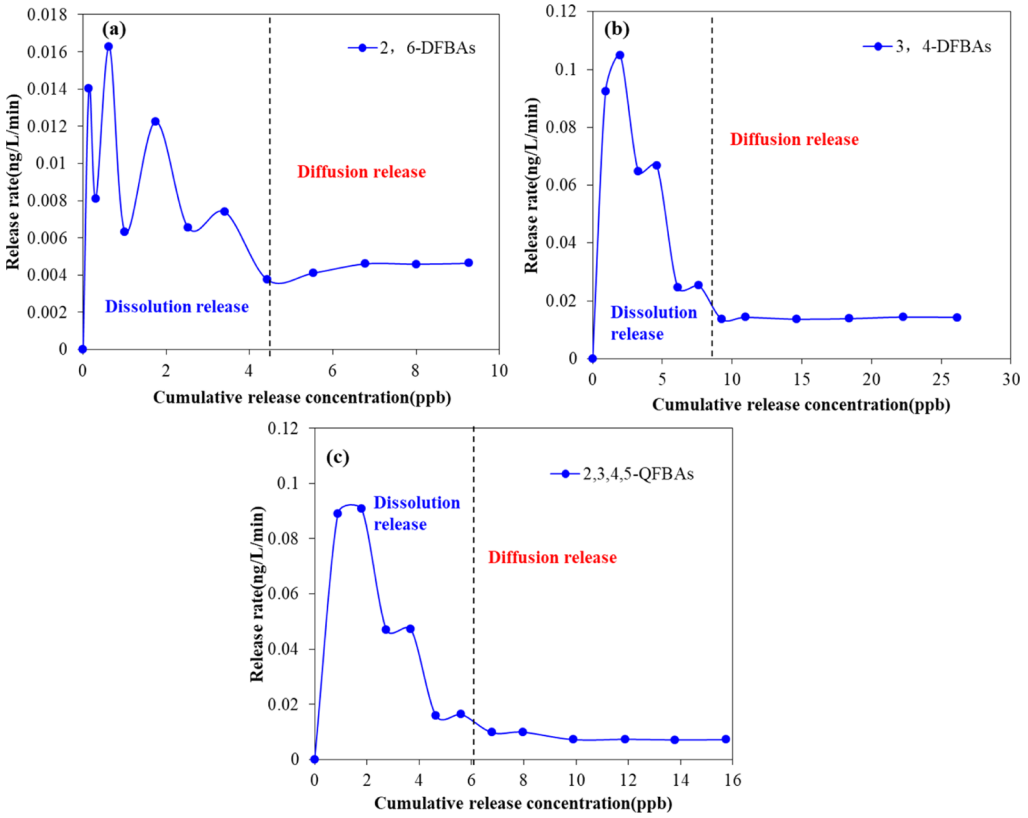

Figure 8. Release rates of sustained-release tracers at different cumulative concentrations. (a) 2,6-difluorobenzoic acid, (b) 3,4-difluorobenzoic acid, and (c) 2,3,4,5-tetrafluorobenzoic acid.

3.3. Release Mechanisms of the Sustained-Release Tracer. The cumulative release concentration of the three sustained-release tracers at normal temperature and in deionized water is shown in Figure 7. According to the experimental results, the release rate of the three tracers is high during the initial stage of the contact with the target fluid and it gradually slows down and becomes stable over time. At the initial stage of contact between the sustained-release tracer and the fluid, the fluid enters into the pores present in the polymer matrix and fills up completely in a short period. Meanwhile, the maximum contact area is achieved between the tracer and the fluid.[33] After complete contact, the tracer mounted on the pore surface of the matrix begins to diffuse rapidly into the water with the shortest diffusion path and the fastest release rate. Over time, the release of the tracers from the surface of the matrix gradually becomes stable, and then, the tracer inside the matrix started getting released and gradually diffused into the fluid. At this time, the path of diffusion becomes longer and the release rate of the tracer material slows down until it becomes stable.[34]

The release mechanism of the sustained-release tracer depends on the interaction between the fluid and the tracer and the time of contact in the fluid. As shown in Figures 8 and 9, there are two processes where the target fluid intrudes into the tracer, corresponding to the two mechanisms of the sustained-release tracer release. The first mechanism is fluid erosion, in which the tracer on the matrix surface gets quickly dissolved into the target fluid when it initially comes in contact with the target fluid. It is a short process and has a fast dissolution rate which decreases rapidly with time. This process can be described using the Noyes−Whitey dissolution equation as shown in eq 1.[34] It could be seen that when the

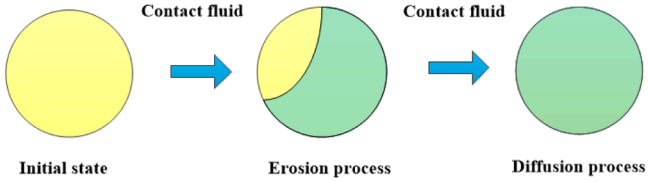

Figure 9. Release process of the sustained-release tracer.

contact area between the tracer and the fluid remains constant and when the tracer is evenly dispersed within the matrix, the release rate of the sustained-release tracer is related to the saturation solubility of the tracer.

$$\frac{dC}{dt} = k_D A(C_s - \rho_{tracer}) \quad (1)$$

where dC/dt is the dissolution rate in g/min, k_D is the dissolution rate constant, A is the surface area of the sustained-release tracer in m2, C_s is the tracer saturation solubility in g/L, and ρ_{tracer} is the tracer mass concentration in g/L.

The second mechanism occurs when the sustained-release tracer is completely coated with the target fluid, that is, the target fluid is filled into polymer matrix pores, and the concentration of tracer increases continuously along with the decrease in the dissolution rate. The dissolution process stops when the tracer concentration approaches the tracer saturation solubility. Then, the sustained-release tracer enters the diffusion release process, which is a slow and continuous process. Over time, the release rate of the tracer tends to become constant. At this time, the cumulative release of the tracer becomes proportional to the contact area of the

https://doi.org/10.1021/acsomega.1c02748
ACS Omega 2021, 6, 19269−19280

sustained-release tracer. The diffusion process is described by the Higuchi diffusion represented using eq 2[35]

$$Q_{tracer} = AD\sqrt{t} \quad (2)$$

where Q_{tracer} is the cumulative diffusion of the tracer in g, D is the diffusion coefficient, and t is the diffusion time in min.

3.4. Effect of Chemistry of the Tracers on the Release Rate. Based on the discussion of the release mechanism in the previous section, we know that the release of the sustained-release tracer is affected by the diffusion coefficient, solubility, contact areas, and contact time of the tracer. The solubility and diffusivity of the three tracers in water are different due to their different chemical properties, so the concentration of the three tracers dissolved in water is highly varying. Figure 8 shows the change in the release rate of the three tracers along with the cumulative release concentration. It is observed that the three sustained-release tracers have different release rates in water. The final stable release rate of the three sustained-release tracers is 0.0045 ppb/min for 2,6-difluorobenzoic acid, 0.014 ppb/min for 3,4-difluorobenzoic acid, and 0.028 ppb/min for 2,3,4,5-tetrafluorobenzoic acid. The water dissolving capacity of the three tracers is in the order of 2,3,4,5-tetrafluorobenzoic acid > 3,4-difluorobenzoic acid > 2,6-difluorobenzoic acid.

3.5. Effect of Temperature and Salinity on the Release Rate. The release performance of sustained -release tracers in the formation environment will change. This is mainly due to the influence of temperature and salinity on the solubility and diffusion coefficient of tracer chemical compositions. Therefore, it is necessary to investigate the influence of formation temperature and formation water salinity on the release capacity of the sustained-release tracer. Figure 10 shows the experimental results of the influence of

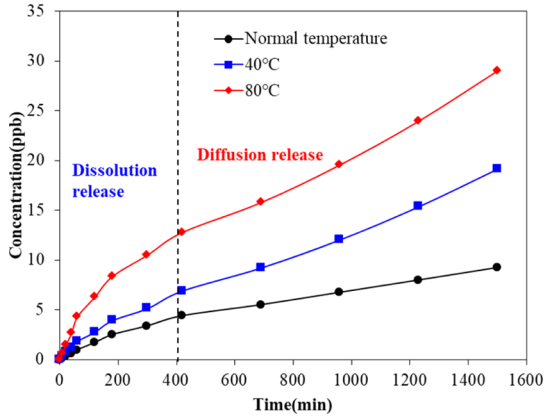

Figure 10. Cumulative release concentration curve of sustained-release tracers at different temperatures (2,6-difluorobenzoic acid).

temperature on the sustained-release performance. It is found that the release rate of the sustained-release tracer increased with the temperature rise. The cumulative release after stabilization at room temperature is equal to 9.67 ppb and increase to 29.32 ppb at 80 °C. The reason for this phenomenon is that temperature affects the diffusion coefficient of the tracer. With the increasing temperature, the diffusion coefficient of tracer increases so that the release rate after stabilization is increased.

Figure 11 shows the tracer release under different salinity conditions. The results show that the salinity has a higher inhibitory effect on the release of the sustained-release tracer

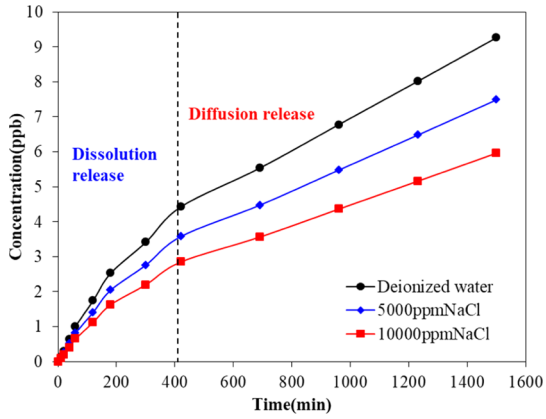

Figure 11. Cumulative release concentration curve of sustained-release tracers under different salinity conditions (2,6-difluorobenzoic acid).

because the salinity is increased from 0 to 10000 ppm and the cumulative release is reduced from 9.67 to 5.92 ppb. Because the fluid salinity reduces the tracer solubility in water, therefore, the higher the salinity, the lower the tracer saturation solubility in water and the lower the cumulative release.

3.6. Effect of the Flow Rate on the Release Rate. The difference in horizontal heterogeneity in the production of horizontal wells resulted in different flow rates in each section, which led to different scour rates for the sustained-release tracers. Figure 12 shows the change in the release rate with

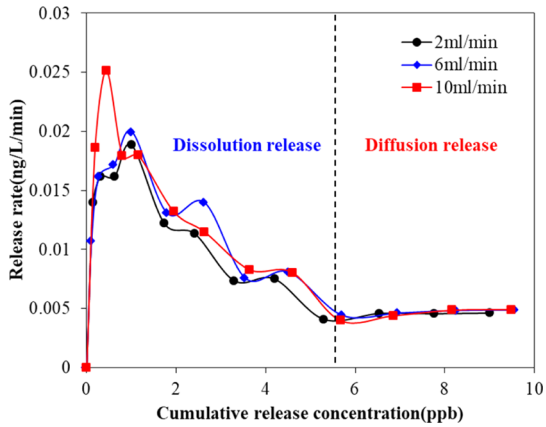

Figure 12. Release rate of the sustained-release tracer at different flow rates (2,6-difluorobenzoic acid).

cumulative release concentration at different flow rates. It can be seen that there is no significant difference in the change in the release rate at different flow rates at the same time and the release rate at a low flow rate is slightly lower than that at a high flow rate. At a high flow rate, the initial release rate is slightly higher than the one at a low flow rate, and over the time, it remains constant after getting stabilized. It is determined that the flow rate has no effect on the release rate of the tracer.

4. FIELD CASE

4.1. Principle of Inflow Profile Monitoring. The sustained-release tracer is commonly used to monitor the inflow profile in horizontal wells with segregated completion. Different types of sustained-release tracers are installed in

https://doi.org/10.1021/acsomega.1c02748
ACS Omega 2021, 6, 19269−19280

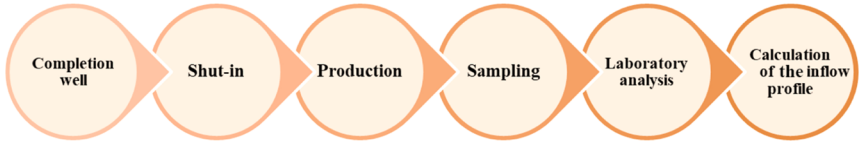

Figure 13. Inflow profile test procedure.

different sections of the horizontal well. During the production of the horizontal well, formation fluids flow into the completion section and come in full contact with the sustained-release tracers installed in the wellbore. The water phase or oil phase in the produced fluid contains special markers after contacting with the tracer, and the samples are collected from the surface for analysis to obtain the contribution from each section of the production.

The experimental results show that the release rate of the sustained-release tracer is not affected by the flow rate but only depends on its properties and the formation environment. The concentration distribution of the tracer in each section does not change under the normal production of the horizontal well, and the inflow profile cannot be obtained. Therefore, the sustained-release tracer interpretation of the inflow profile requires a special approach in which the theoretical basis involves the dissolution and diffusion mechanism of the tracer and the single-phase flow theory of the horizontal well. Based on this, the inflow profile process of the sustained-release tracer testing is divided into five steps (Figure 13): ① Initial state. ② Shut-in. ③ Well sampling. ④ Analysis of samples. ⑤ Inflow profile interpretation.

4.2. Inflow Profile Interpretation. *4.2.1. Design and Installation of the Sustained-Release Tracer.* The horizontal well X is located on an offshore platform. The reservoir heterogeneity in the horizontal section of the well is strong and has a large range of permeability. The permeability in the heel and toe section is about 13,000 mD, whereas, in the middle section, it was about 4000 mD. Currently, the well produces about 600 m^3/d of fluid and less than 10 m^3/d of oil, with water cuts as high as 98%. Because of the high water cut in the horizontal well X, the intelligent water-controlled completion string is chosen to enhance oil recovery. The intelligent water-controlled completion string is structured using downhole packers to separate the horizontal section into three sections, each containing an active water-controlled switch, an AICD nipple, and the sustained-release tracers. The sustained-release tracers prepared in this study are installed to monitor the inflow profile of the horizontal well X. Table 3 shows the installation parameters of the three sustained-release tracers. Figure 14 shows the locations of three tracers installed at the downhole. The formation temperature of the well X is about 65 °C, and the salinity of the produced water is about 7100 ppm. The experimental results based on the factors affecting the release of the sustained-release tracer show that the three tracers can work in the formation environment.

Table 3. Installation Parameters of the Sustained-Release Tracers

completion section	horizontal position	tracer	number	material
First	1810.045 m	tracer-1	12	2,6-difluorobenzoic acid
Second	2008.24 m	tracer-2	24	3,4-difluorobenzoic acid
Third	2019.176 m	tracer-3	12	2,3,4,5-tetrafluorobenzoic acid

4.2.2. Inflow Profile Interpretation and Verification. The interpretation model of the sustained-release tracer inflow profile is obtained using the time taken by the peak tracer concentration to arrive at the wellhead and the difference in the wellbore volume between the sections of the tracer system. This method requires a well shut-in before sampling, which aims to allow the fluid flowing out of each section to come in contact with the sustained-release tracers and to release a high concentration of the tracer near the wellbore. Due to the downhole packer, the horizontal flow is avoided and the flow into the wellbore in each section is only in contact with the sustained-release tracers that are installed in the section, thereby ensuring the accuracy of the sustained-release tracer labeling.

It is assumed that the highly concentrated tracer near the wellbore is transported to the wellhead sampling point in the form of a slug after restart and there would be no diffusion or settlement during the migration process. The arrival time taken by the highly concentrated tracer slug to reach the wellhead during balanced production can be calculated according to the wellbore inflow model. However, due to the difference in production in each section, the real arrival time of the highly concentrated tracer slug to the wellhead deviates from the theoretical time of simulating balanced production. There is a functional relationship between the actual flow and the real arrival time of the highly concentrated tracer slug. The real time peak tracer concentration arriving at the wellhead in each section can be obtained through a sampling test. Figure 15 shows the relationship between the wellbore volume, the flow rate of each section, and the arrival time of various tracers. The total flow rate can be calculated from the time of peak tracer concentration in the first section (heel section) to the wellhead. At the same time, the flow rate from the second section to the final section can be calculated from the time of peak tracer concentration in the second section to the wellhead. By analogy, the flow rate in each section can be calculated. This interpretation model is called the arrival time model, as shown in eqs 3−5

$$q_t = \sum_{i=1}^{n} q_i \tag{3}$$

$$V = \sum_{i=1}^{n} V_i \tag{4}$$

https://doi.org/10.1021/acsomega.1c02748
ACS Omega 2021, 6, 19269−19280

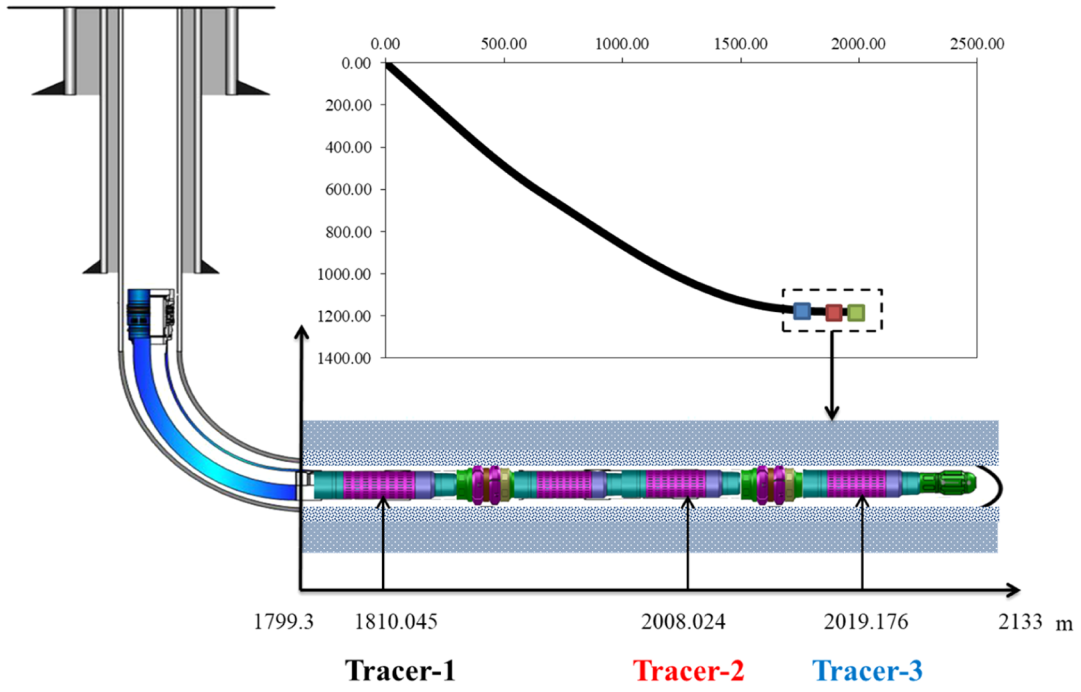

Figure 14. Sustained-release tracer installation location in the horizontal section of the well X.

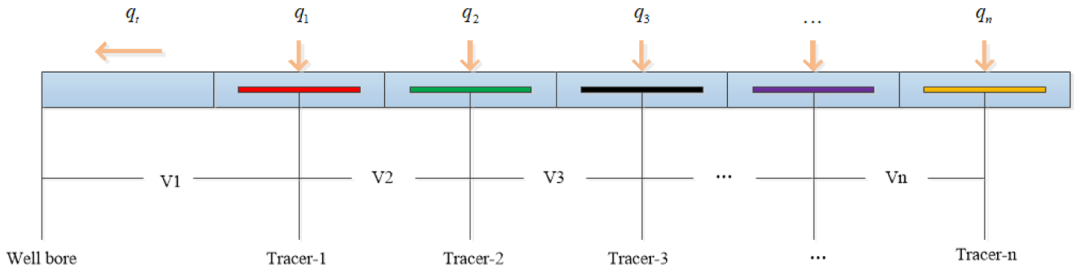

Figure 15. Fluid inflow profile interpretation model.

$$\begin{cases} q_t = \dfrac{V_1}{t_1} \\ q_t - q_1 = \dfrac{V_2}{t_2 - t_1} \\ q_t - q_1 - q_2 = \dfrac{V_3}{t_3 - t_2} \\ \cdots \\ q_t - q_1 - q_2 \cdots - q_{i-1} = \dfrac{V_i}{t_i - t_{i-1}} \end{cases} \quad (5)$$

where q_i is the production flow rate of period i in m^3/d, q_t is the total fluid flow rate in m^3/d, V_1 is the volume from the first section to the wellhead in m^3, V_i (i = 2, 3, 4...n) is the wellbore volume between period i and i−1 in m^3/d, V is the total wellbore volume in m^3, and t_i and t_{i-1} are the time of the peak tracer concentration flow to the wellhead in period i and i_1 min, respectively.

The sample test results for both times are shown in Figures 16 and 17. The first time is the initial state and the second time is the adjusted state of the active water-controlled switch. As shown in Figures 16 and 17, there are horizontal differences in the tracer concentrations among the three tracer systems. In order to compare the response shapes of each tracer system in a better way, the two test results are normalized (by dividing all the tracer concentrations for a given tracer by the peak of the tracer system so that all the response values were between 0 and 1). The real time when the peak tracer concentration arrived at the wellhead is determined from test results. The parameters (Table 4) required by the inflow profile interpretation model, such as the arrival time and wellbore volume, are substituted in the model to calculate the contribution of each section during the two sampling tests.

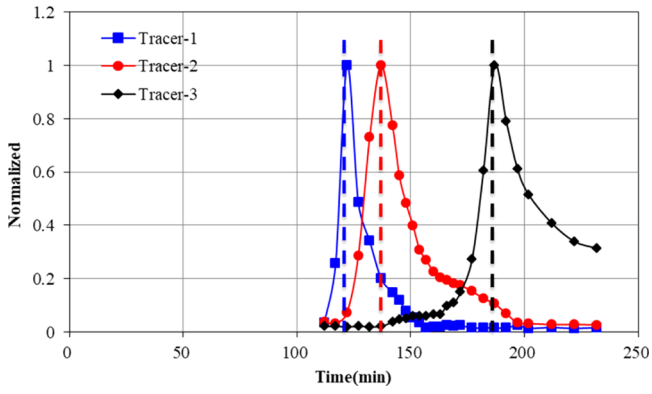

Figure 16. Tracer concentration normalization curve for the first sample.

https://doi.org/10.1021/acsomega.1c02748
ACS Omega 2021, 6, 19269−19280

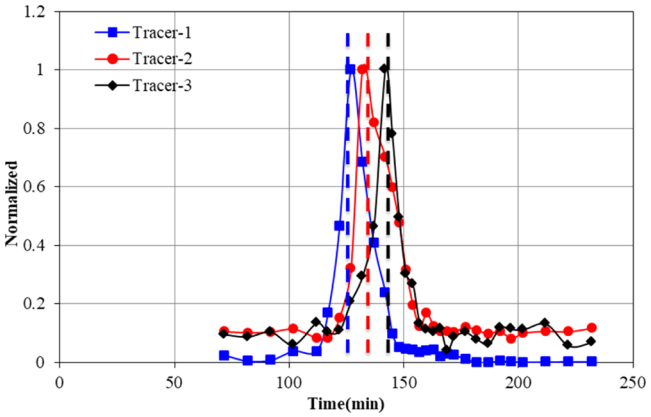

Figure 17. Tracer concentration normalization curve for the second sample.

Table 4. Inflow Profile Interpretation Model Parameters

sampling	tracer type	peak tracer time to wellhead (min)	volume (m^3)
First	tracer-1	122	18.2
	tracer-2	137	18.4
	tracer-3	187	18.75
Second	tracer-1	127	18.2
	tracer-2	130	18.4
	tracer-3	138	18.75

Figure 18 shows the comparison of production contributions of each section before and after the active water-controlled switch adjustment. It is observed that before the active water-controlled switch adjustment, the production contribution of the heel section is the largest, which accounted for 88.57% of production. The water supplying capacity of the middle and toe section is weak and the production is only 5.43 and 6%, respectively. After the adjustment of the active water-controlled switch, the water cut decreased to 93% and the inflow profile of the horizontal section is modified. At this time, the production contribution of the heel section is decreased to 50%, while the production contribution of the middle and toe section increased to 17.19 and 32.81%, respectively, indicating that the active water control adjustment balanced out the contribution of production in each section and improved the supply capacity of the low-production section.

To verify the reliability of the interpretation results, this study used the commercial software (Eclipse2011) to simulate the contribution of each section in the production of the well in the two-sampling point water control state. The calculation results show that the production contribution of each section of the well X under the first sampling condition is 79.35, 9.08, and 11.57% (Figure 19). In the second sampling, the production contribution of each section is 49.36, 15.69, and 34.93%, which is similar to the interpretation results of the sustained-release tracer, verifying the reliability and accuracy of the sustained-release tracer interpretation of the inflow profile.

5. CONCLUSIONS

In summary, three kinds of water-soluble solid sustained-release tracers were developed to effectively monitor the inflow profile of the horizontal wells. Their preparation methods, release mechanisms, and detection methods were studied experimentally. Finally, the monitoring technology of the sustained-release tracer inflow profile was tested in the well X in an offshore oil field. The inflow profile of the well X was quantitatively interpreted through a specific interpretation method of the inflow profile. The main conclusions were as follows:

1. Using bisphenol A epoxy resin as the skeleton and 2,6-difluorobenzoic acid, 3,4-difluorobenzoic acid, and 2,3,4,5-tetrafluorobenzoic acid as tracers, a stable sustained-release tracer was obtained through high-temperature curing. This tracer had a single sensitivity and could be released in water, but it was inert in oil. The tracer was evenly distributed in the skeleton and had stable release performance after being in contact with water. The release rate of the sustained-release tracer was affected by the underground environment. The higher the temperature was, the faster the release rate was, while the higher the salinity was, the slower the release rate was. The flow rate had no eminent effect on the release rate.
2. An interpretation model for monitoring the fluid inflow profile with the sustained-release tracer was established. The model calculated the contribution of the fluid production in each section according to the peak time of the tracer group arrived at the wellhead after the well reopening and the single-phase wellbore flow simulation. Application of the interpretation model of the well X

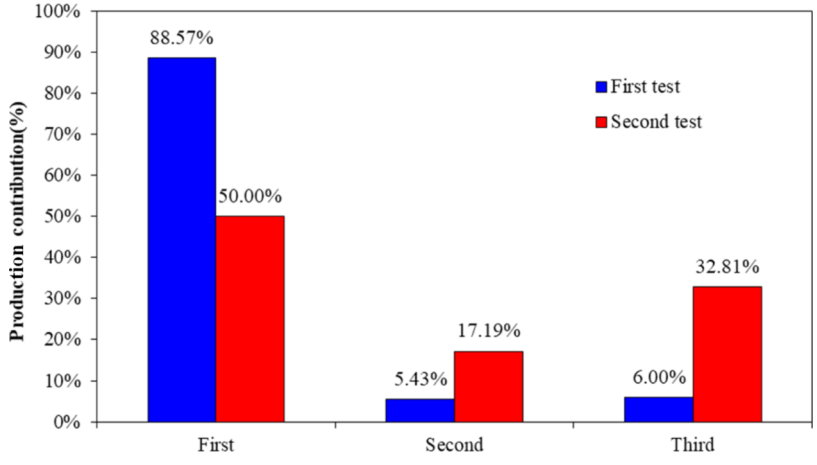

Figure 18. Interpretation results of production contribution in two tests of well X.

https://doi.org/10.1021/acsomega.1c02748
ACS Omega 2021, 6, 19269−19280

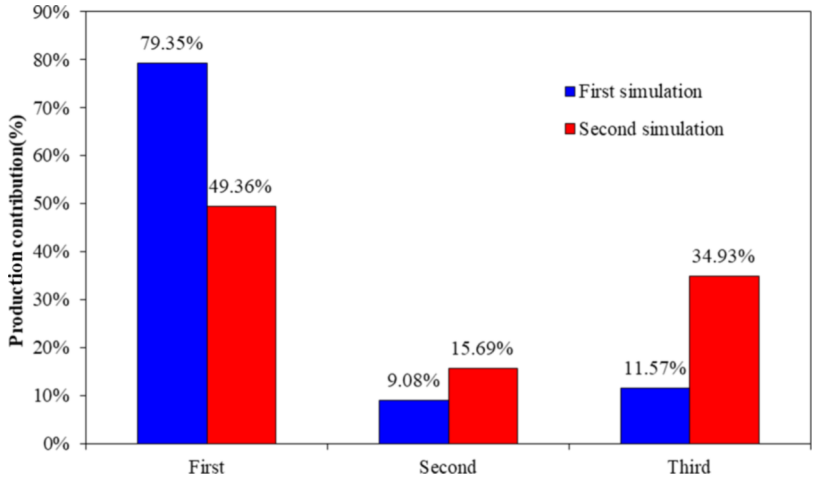

Figure 19. Simulation results of production contribution in two tests of well X.

before and after the two adjustments of the water control switch and the quantitative interpretation of the liquid profile were made, and the interpretation results showed that before the adjustment of the water control switch, the fluid production contribution of the heel, middle, and toe section was 88.57, 5.43, and 6.00%, respectively. The liquid production contributions of the heel, middle, and toe section after the adjustment of the water control switch were 50.00, 17.19, and 32.81%, respectively, indicating that the adjusted water control switch played a role in improving the liquid production contribution.

AUTHOR INFORMATION

Corresponding Author

Zimin Liu − *State Key Laboratory of Oil and Gas Reservoir Geology and Exploitation, Southwest Petroleum University, Chengdu, Sichuan 610500, PR China;* orcid.org/0000-0002-1106-5104; Email: dmlwasas@163.com

Authors

Haitao Li − *State Key Laboratory of Oil and Gas Reservoir Geology and Exploitation, Southwest Petroleum University, Chengdu, Sichuan 610500, PR China*

Ying Li − *State Key Laboratory of Oil and Gas Reservoir Geology and Exploitation, Southwest Petroleum University, Chengdu, Sichuan 610500, PR China*

Hongwen Luo − *State Key Laboratory of Oil and Gas Reservoir Geology and Exploitation, Southwest Petroleum University, Chengdu, Sichuan 610500, PR China*

Xiaojiang Cui − *State Key Laboratory of Oil and Gas Reservoir Geology and Exploitation, Southwest Petroleum University, Chengdu, Sichuan 610500, PR China;* orcid.org/0000-0002-4571-9524

Song Nie − *State Key Laboratory of Oil and Gas Reservoir Geology and Exploitation, Southwest Petroleum University, Chengdu, Sichuan 610500, PR China*

Kairui Ye − *Shale Gas Exploration & Development Project Department of Chuanqing Drilling Engineering CO. Ltd., CNPC, Chengdu, Sichuan 610051, PR China*

Complete contact information is available at: https://pubs.acs.org/10.1021/acsomega.1c02748

Notes

The authors declare no competing financial interest.

ACKNOWLEDGMENTS

This research was supported by the National Science and Technology Major Project (grant no. 2016ZX05058003−022). We also appreciate Dr. Bo Gao from the Analytical & Testing Center of Sichuan University for helping with UPLC-MS characterization.

REFERENCES

(1) Ronaldo, V.; Cem, S.; Turgay, E. *Horizontal Well Design Optimization: A Study of the Parameters Affecting the Productivity and Flux Distribution of a Horizontal Well*, SPE Annual Technical Conference and Exhibition, 2003.

(2) Durlofsky, L. J. An Approximate Model for Well Productivity in Heterogeneous Porous Media. *Math. Geol.* **2000**, *32*, 421−438.

(3) Zhang, N.; Li, H.; Liu, Y.; Shan, J.; Tan, Y.; Li, Y. A new autonomous inflow control device designed for a loose sand oil reservoir with bottom water. *J. Pet. Sci. Eng.* **2019**, *178*, 344−355.

(4) Huang, S.; Zhu, Y.; Ding, J.; Li, X.; Xue, Y. A semi-analytical model for predicting inflow profile of long horizontal wells in super-heavy foamy oil reservoir. *J. Pet. Sci. Eng.* **2020**, *195*, 107952.

(5) Li, H.; Tan, Y.; Jiang, B.; Wang, Y.; Zhang, N. A semi-analytical model for predicting inflow profile of horizontal wells in bottom-water gas reservoir. *J. Pet. Sci. Eng.* **2018**, *160*, 351−362.

(6) Luo, W.; Li, H.-T.; Wang, Y.-Q.; Wang, J.-C. A new semi-analytical model for predicting the performance of horizontal wells completed by inflow control devices in bottom-water reservoirs. *J. Nat. Gas Sci. Eng.* **2015**, *27*, 1328−1339.

(7) Wilson, A. Production-Logging Tools Facilitate Well Testing in Challenging Environments. *J. Pet. Technol.* **2016**, *68*, 79−80.

(8) Bilinchuk, A. V.; Ipatov, A. I.; Ipatov, A. I.; Kremenetskiy, M. I.; Sitnikov, A. N.; Yakovlev, A. A.; Shurunov, A. V.; Galeev, R. R.; Kolesnikov, M. V. Evolution of production logging in low permeability reservoirs at horizontal wells, multiple-fractured horizontal wells and multilateral wells. Gazprom Neft experience. *Neft. khozyaystvo - Oil Ind.* **2018**, *2018*, 34−37.

(9) App, J. Permeability, Skin, and Inflow-Profile Estimation From Production-Logging-Tool Temperature Traces. *SPE J.* **2017**, *22*, 1123−1133.

(10) Luo, H.; Li, H.; Tan, Y.; Li, Y.; Jiang, B.; Lu, Y.; Cui, X. A novel inversion approach for fracture parameters and inflow rates diagnosis in multistage fractured horizontal wells. *J. Pet. Sci. Eng.* **2020**, *184*, 106585.

(11) Luo, H.; Li, Y.; Li, H.; Cui, X.; Chen, Z. Simulated Annealing Algorithm-Based Inversion Model To Interpret Flow Rate Profiles

and Fracture Parameters for Horizontal Wells in Unconventional Gas Reservoirs. *SPE J.* **2021**, 1−21.
(12) Denney, D. Alkaline/Surfactant/Polymer Flood: Single-Well Chemical-Tracer Tests - Design, Implementation, and Performance. *J. Pet. Technol.* **2011**, *63*, 86−88.
(13) Jin, L.; Jamili, A.; Harwell, J. H.; Shiau, B. J.; Roller, C. *Modeling and Interpretation of Single Well Chemical Tracer Tests (SWCTT) for pre and post Chemical EOR in two High Salinity Reservoirs*, SPE Production and Operations Symposium, 2015.
(14) Khaledialidusti, R.; Kleppe, J. Surface-Charge Alteration at the Carbonate/Brine Interface During Single-Well Chemical-Tracer Tests: Surface-Complexation Model. *SPE J.* **2018**, *23*, 2302−2315.
(15) Silva, M.; Stray, H.; Bjørnstad, T. Stability assessment of PITT tracer candidate compounds − The case of pyrazines. *J. Pet. Sci. Eng.* **2019**, *182*, 106269.
(16) Al-Murayri, M. T.; Al-Qenae, A.; AlRukaibi, D.; Chatterjee, M.; Hewitt, P. *Design of a Partitioning Interwell Tracer Test for a Chemical EOR Pilot Targeting the Sabriyah Mauddud Carbonate Reservoir in Kuwait*, SPE Kuwait Oil & Gas Show and Conference, 2017.
(17) Ghergut, I.; Behrens, H.; Sauter, M. Tracer-based Quantification of Individual Frac Discharge in Single-well Multiple-frac Backflow: Sensitivity Study. *Energy Procedia* **2014**, *59*, 235−242.
(18) Li, L.; Jiang, H.; Li, J.; Wu, K.; Meng, F.; Chen, Z. Modeling tracer flowback in tight oil reservoirs with complex fracture networks. *J. Pet. Sci. Eng.* **2017**, *157*, 1007−1020.
(19) Tian, W.; Wu, X.; Shen, T.; Kalra, S. Estimation of hydraulic fracture volume utilizing partitioning chemical tracer in shale gas formation. *J. Nat. Gas Sci. Eng.* **2016**, *33*, 1069−1077.
(20) Fu, Y.; Dehghanpour, H. How far can hydraulic fractures go? A comparative analysis of water flowback, tracer, and microseismic data from the Horn River Basin. *Mar. Pet. Geol.* **2020**, *115*, 104259.
(21) Dyrli, A. D.; Leung, E. *Ten Years of Reservoir Monitoring with Chemical Inflow Tracers - What Have We Learnt and Applied Over the Past Decade?*, SPE Kuwait Oil & Gas Show and Conference, 2017.
(22) Carpenter, C. Lessons From 10 Years of Monitoring With Chemical Inflow Tracers. *J. Pet. Technol.* **2018**, *70*, 81−83.
(23) Andresen, C.; Williams, B.; Morgan, M.; Williams, T.; Crumrine, T.; Bond, A.; Franks, J. *Interventionless Surveillance in a Multi-Lateral Horizontal Well*; IADC/SPE Drilling Conference and Exhibition, 2012.
(24) Montes, A.; Nyhavn, F.; Oftedal, G.; Fævelen, E.; Andresen, C.; Leung, E.; Wikmark, V. *Application of Inflow Well Tracers for Permanent Reservoir Monitoring in North Amethyst Subsea Tieback ICD wells in Canada*; SPE Middle East Intelligent Energy Conference and Exhibition, 2013.
(25) Qamber, A.; Hassan, M.; Ali, A. *The Application of Chemical Tracer Monitoring in Multi Stage Acid Frac Wells in the Mature Bahrah Field, North Kuwait*; SPE Kuwait Oil & Gas Show and Conference, 2019.
(26) Semikin, D.; Senkov, A.; Surmaev, A.; Prusakov, A.; Leung, E. *Autonomous ICD Well Performance Completed With Intelligent Inflow Tracer Technology in the Yuri Korchagin Field in Russia*; SPE Russian Petroleum Technology Conference, 2015.
(27) Anopov, A.; Ovchinnikov, K.; Katashov, A. *Production Logging Using Quantum Dots Tracers®*; SPE Middle East Oil and Gas Show and Conference, 2019.
(28) Napalowski, R.; Loro, R.; Anderson, C.; Andresen, C.; Dyrli, A. D.; Nyhavn, F. *Successful Application of Well Inflow Tracers for Water Breakthrough Surveillance in the Pyrenees Development, Offshore Western Australia*; SPE Asia Pacific Oil and Gas Conference and Exhibition, 2012.
(29) Spilker, K. K.; Dwarakanath, V.; Malik, T.; Burdett Tao, E.; Mirkovic, Z. *Characterizing Tracer Applicability in Different Mineralogy*; SPE Improved Oil Recovery Conference, 2016.
(30) AlAbbad, M. A.; Sanni, M. L.; Kokal, S.; Krivokapic, A.; Dye, C.; Dugstad, Ø.; Hartvig, S. K.; Huseby, O. K. A Step Change for Single-Well Chemical-Tracer Tests: Field Pilot Testing of New Sets of Novel Tracers. *SPE Reservoir Eval. Eng.* **2019**, *22*, 253−265.
(31) Silva, M.; Bjørnstad, T. Determination of phase-partitioning tracer candidates in production waters from oilfields based on solid-phase microextraction followed by gas chromatography-tandem mass spectrometry. *J. Chromatogr. A* **2020**, *1629*, 461508.
(32) Serres-Piole, C.; Preud'homme, H.; Moradi-Tehrani, N.; Allanic, C.; Jullia, H.; Lobinski, R. Water tracers in oilfield applications: Guidelines. *J. Pet. Sci. Eng.* **2012**, *98*−*99*, 22−39.
(33) Sackett, C. K.; Narasimhan, B. Mathematical modeling of polymer erosion: Consequences for drug delivery. *Int. J. Pharm.* **2011**, *418*, 104−114.
(34) Li, S.; Shen, Y.; Li, W.; Hao, X. A common profile for polymer-based controlled releases and its logical interpretation to general release process. *J. Pharm. Pharm. Sci.* **2006**, *9*, 238−244.
(35) Higuchi, T. Mechanism of sustained-action medication. Theoretical analysis of rate of release of solid drugs dispersed in solid matrices. *J. Pharm. Sci.* **1963**, *52*, 1145−1149.

https://doi.org/10.1021/acsomega.1c02748
ACS Omega 2021, 6, 19269−19280